Shock-induced phase transition in systems of hard spheres with internal degrees of freedom

Shigeru Taniguchi,[1] Andrea Mentrelli,[2] Nanrong Zhao,[3] Tommaso Ruggeri,[2] and Masaru Sugiyama[1]
[1]*Graduate School of Engineering, Nagoya Institute of Technology, Nagoya 466-8555, Japan*
[2]*Department of Mathematics & Research Center of Applied Mathematics (CIRAM), University of Bologna, Bologna, Italy*
[3]*College of Chemistry, Sichuan University, Chengdu 610064, People's Republic of China*

(Received 26 March 2010; published 16 June 2010)

Shock waves and shock-induced phase transitions are theoretically and numerically studied on the basis of the system of Euler equations with caloric and thermal equations of state for a system of hard spheres with internal degrees of freedom. First, by choosing the unperturbed state (the state before the shock wave) in the liquid phase, the Rankine-Hugoniot conditions are studied and their solutions are classified on the basis of the phase of the perturbed state (the state after the shock wave), being a shock-induced phase transition possible under certain conditions. With this regard, the important role of the internal degrees of freedom is shown explicitly. Second, the admissibility (stability) of shock waves is studied by means of the results obtained by Liu in the theory of hyperbolic systems. It is shown that another type of instability of a shock wave can exist even though the perturbed state is thermodynamically stable. Numerical calculations have been performed in order to confirm the theoretical results in the case of admissible shocks and to obtain the actual evolution of the wave profiles in the case of inadmissible shocks (shock splitting phenomena).

DOI: 10.1103/PhysRevE.81.066307 PACS number(s): 47.40.−x, 64.70.D−, 62.50.Ef

I. INTRODUCTION

Shock waves, which are characterized by the steep and rapid changes in physical quantities such as mass density, velocity, temperature, and pressure at a shock front, are typical nonlinear waves that have been studied from many aspects experimentally, theoretically, and numerically. From a theoretical point of view, because of their highly nonlinear and nonequilibrium features, the study of shock waves affords us with fundamental and wide variety of knowledge in the theories of nonlinear wave propagation [1,2] and of nonequilibrium thermodynamics and statistical physics [3–5].

Compared to shock waves in gases [6], shock waves in condensed matters, namely, liquids and solids, have been given much less attention. In recent years, however, shock wave phenomena in condensed matters have attracted much interest of researchers in various fields. See, for example, the review paper [7] and books [8–16] and references cited therein. Among the various phenomena, dynamic phase transitions induced by shock waves are worthy of special attention because these phenomena are not yet well understood although their potential importance in various applications is evident. Material synthesis, for example, sometimes makes use of such dynamic phase transitions [17].

Several studies of the shock-induced phase transitions were made by experiments [18–22] or by computer simulations of microscopic models [23–28]. Some theoretical studies were also made by using the models with realistic interatomic potentials [7,29–31]. However, most of the previous works are based on more or less qualitative models. Therefore, quantitative study of the shock-induced phase transitions is highly expected for the deeper understanding of the phenomena.

In a previous paper [32] (hereafter referred to as paper I), dynamic phase transition induced by a shock wave was studied quantitatively on the basis of the system of Euler equations with caloric and thermal equations of state for a hard-sphere system in which the first-order phase transition (*Alder transition*) can be observed [33–35]. Rankine-Hugoniot (RH) conditions were analyzed in detail and the classification of Hugoniot types in terms of the thermodynamic quantities of the unperturbed state (the state before a shock wave) and of the shock strength was made. The admissibility (stability) of a shock wave was discussed from the viewpoint of the mathematical theory of hyperbolic systems. The importance of a hard-sphere system resides in the fact that it is a suitable reference system for studying shock wave phenomena including the shock-induced phase transitions in more realistic condensed matters with both attractive and repulsive parts of interatomic potential by using the perturbation theory of liquid-state physics [36–38]. In paper I, for simplicity, any internal motion in the constituent hard-sphere particles was neglected.

In the present paper, which is the sequel to paper I, we extend our study by introducing internal degrees of freedom in hard-sphere particles. It is well known that the ultimate compression ratio, i.e., the ratio of mass densities before and after a shock in the strong shock limit, depends strongly on the internal degrees of freedom. In order to show the crucial importance of the internal degrees of freedom on shock-induced phase transitions, we may consider the possibility of shock-induced gas-liquid phase transitions. In Sec. 132 of Ref. [6], the authors expressed their negative opinion about this possibility by saying that "[the compression of gas in an ordinary shock wave] cannot lead to condensation, since the increase of pressure in the shock wave has less effect on the degree of supersaturation than the increase of temperature." Shock-induced gas-liquid phase transitions, however, can be observed in some materials if unperturbed states are suitably chosen [39,40]. Existence of shock-induced gas-liquid phase transitions can also be shown theoretically in a real gas model such as van der Waals gas, *if the constituent molecules have suitably many internal degrees of freedom* and if unperturbed states are suitably taken [41]. Roughly speaking, because of the energy flow into the internal motion, the increase in temperature of such a gas due to a shock compression is comparatively small, and then a gas-liquid phase transition may occur more easily. We naturally expect that the internal degrees of freedom have similar effects also on liquid-solid phase transitions, especially on Alder transition in a hard-sphere system. We will see below that our expectation is quite relevant.

The purpose of the present paper is to study shock wave phenomena in a hard-sphere system with internal motion both theoretically and numerically. To be more specific, we will study the following three points in detail: (i) the dependence of the solution of RH conditions on the internal degrees of freedom of a hard-sphere system, (ii) the admissibility of shock waves, and (iii) the effects of the internal degrees of freedom on shock-induced phase transitions.

II. BASIC EQUATIONS

In this section, we summarize the basic equations of the hard-sphere system model. We consider hard spheres in a three-dimensional space, but we study shock-induced phase transitions and shock admissibility focusing on one-dimensional waves (plane waves) traveling only along the x direction. Therefore, the system of equations that we study is written in the one-dimensional case but the equations of state are written assigning to the hard spheres three degrees of freedom connected to the translational motion.

A. Caloric and thermal equations of state

We adopt the following caloric equation of state:

$$e = \frac{\mathcal{D}}{2m} k_B T, \tag{1}$$

where e, $\mathcal{D}$, m, k_B, and T are the specific internal energy, the degrees of freedom of a hard-sphere particle, the mass of a particle, the Boltzmann constant, and the absolute temperature, respectively. The degrees of freedom, $\mathcal{D}$, is the sum of the space dimensionality (3 in our analysis), corresponding to the degrees of freedom of the translational motion of a particle and the internal degrees of freedom of a particle, f, so

$$\mathcal{D} \equiv 3 + f. \tag{2}$$

Note that the internal degrees of freedom, f, corresponds to the number of excited eigenmodes of internal motion in a particle and it is assumed to be constant. In the derivation of Eq. (1), we have assumed that all the excited modes satisfy the equipartition law of energy in classical statistical mechanics. Although these assumptions are very strong, we believe that they are appropriate as a first step in our analysis. The results obtained below will show us a sound direction for the next steps of this study.

As in paper I, the thermal equation of state is given by

$$\frac{p\omega}{k_B T} = \eta \Gamma(\eta), \quad \Gamma(\eta) \equiv 1 + \chi(\eta), \tag{3}$$

where p is the pressure, $\chi(\eta)$ is the deviation from the ideal gas law, and η is the packing fraction related to the mass density ρ by

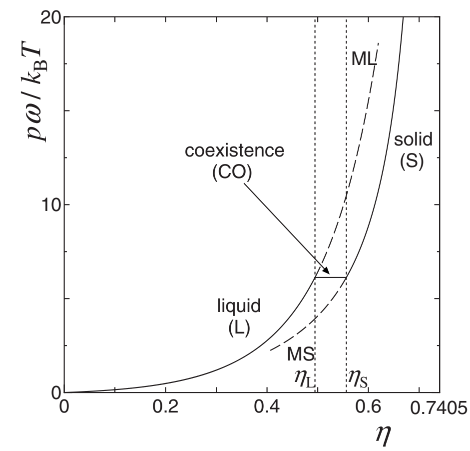

FIG. 1. Liquid phase and solid phase branches of the $p\omega/k_BT$-η curve for a hard-sphere system (L: stable liquid branch; ML: metastable liquid branch; S: stable solid branch, MS: metastable solid branch; CO: liquid-solid coexistence branch). η_L and η_S are the packing fractions at the freezing and melting points, respectively.

$$\eta \equiv \frac{\rho\omega}{m},$$

with ω being the volume of a hard sphere ($\omega = \pi\sigma^3/6$, where σ is the diameter of a hard sphere). We adopt the Padé approximation $[P(3,3)]$ for the liquid phase [42] and the results from the free volume theory for the solid phase [36] as follows:

$$\chi^L(\eta) = \frac{4\eta + 1.016\,112\eta^2 + 1.109\,056\eta^3}{1 - 2.245\,972\eta + 1.301\,008\eta^2},$$

$$\chi^S(\eta) = \frac{1}{\left(\frac{\sqrt{2}\pi}{6\eta}\right)^{1/3} - 1},$$

where superscripts L and S stand for the liquid and solid phases, respectively. Hereafter we also use these superscripts for the quantity Γ as follows:

$$\Gamma^L(\eta) \equiv 1 + \chi^L(\eta), \quad \Gamma^S(\eta) \equiv 1 + \chi^S(\eta).$$

As seen in Fig. 1, the curve $p\omega/k_BT$-η has two branches: one is the liquid phase branch and the other one is the solid phase branch. Both branches have thermodynamically metastable parts (ML and MS) as well as stable parts (L and S). The packing fractions η_L and η_S are, respectively, the values of η at the freezing point and at the melting point. In the range between η_L and η_S, there can be liquid-solid coexistence states (CO) with a common temperature T^* and a common pressure p^*. According to the simulation data [35],

$$\frac{6}{\sqrt{2}\pi} \frac{p^*\omega}{k_B T^*} \approx 8.27,$$

and the values of η_L and η_S are given by

$$\eta_L \approx 0.4946, \quad \eta_S \approx 0.5564.$$

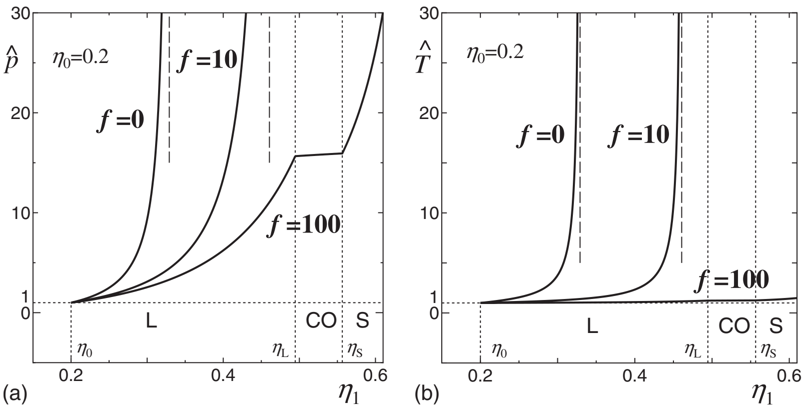

FIG. 2. Hugoniot loci, represented in the $\hat{p}$-η_1 and $\hat{T}$-η_1 planes, for three different values of the internal degrees of freedom f $(f=0,10,100)$. In the case $f=100$, the Hugoniot loci cross the coexistence region, going from the liquid phase region to the solid phase region, as the shock strength increases (case P-2). The unperturbed packing fraction is $\eta_0=0.2$. Vertical dashed lines are asymptotes, $\eta_1=\eta_1^{\infty}$, for $f=0,10$.

As we have seen in this section, the only difference between the basic equations adopted here and those introduced in paper I is in the expression of the caloric equation of state [Eq. (1)]. This seemingly small difference, however, leads to some profound differences in shock wave phenomena as seen in the following.

B. System of Euler equations

The system of Euler equations describing the conservation of mass, momentum, and energy for a compressible fluid in the one-dimensional case can be expressed as

$$\mathbf{u}_t + \mathbf{F}_x(\mathbf{u}) = 0, \tag{4}$$

where the subscripts (time t and position x) denote partial differentiation. Here, the density $\mathbf{u}$ and the flux $\mathbf{F}$ are given by

$$\mathbf{u} = \begin{pmatrix} \rho \\ \rho v \\ \rho e + \frac{1}{2}\rho v^2 \end{pmatrix}, \quad \mathbf{F} = \begin{pmatrix} \rho v \\ \rho v^2 + p \\ \left(\rho e + \frac{1}{2}\rho v^2 + p\right) v \end{pmatrix}, \tag{5}$$

with v being the velocity. The characteristic velocities of the hyperbolic system (4) and (5) are given by

$$\lambda_1 = v - c, \quad \lambda_2 = v, \quad \lambda_3 = v + c,$$

where $c=\sqrt{(\partial p/\partial \rho)_s}$ represents the sound velocity and s is the specific entropy.

III. RANKINE-HUGONIOT CONDITIONS

The system of Euler equations (4) and (5) admits a plane shock wave provided that the jump of the physical quantities between the states before and after the shock front satisfies the well-known RH conditions,

$$-U_s[\![\mathbf{u}]\!] + [\![\mathbf{F}(\mathbf{u})]\!] = 0, \tag{6}$$

where U_s is the propagation velocity of the shock front and $[\![\psi]\!]=\psi_1-\psi_0$ represents the jump of a generic quantity ψ across the shock front, with ψ_1 being the quantity in the state after the shock (*perturbed state*) and ψ_0 in the state before the shock (*unperturbed state*). Conditions (6) are explicitly written by using the packing fraction η instead of the mass density ρ as follows:

$$-U_s[\![\eta]\!] + [\![\eta v]\!] = 0,$$

$$-U_s[\![\eta v]\!] + \left[\!\!\left[\eta v^2 + \frac{p\omega}{m}\right]\!\!\right] = 0,$$

$$-U_s\left[\!\!\left[\eta e + \frac{1}{2}\eta v^2\right]\!\!\right] + \left[\!\!\left[\left(\eta e + \frac{1}{2}\eta v^2 + \frac{p\omega}{m}\right)v\right]\!\!\right] = 0. \tag{7}$$

The Mach number in the unperturbed state, M_0, is defined by

$$M_0 \equiv \frac{U_s - v_0}{c_0},$$

where the quantities with the subscript 0 are the so-called *unperturbed quantities*, i.e., the quantities evaluated in the unperturbed state (analogously, the quantities with the subscript 1 are evaluated in the perturbed state and are called *perturbed quantities*). In the present case, we have

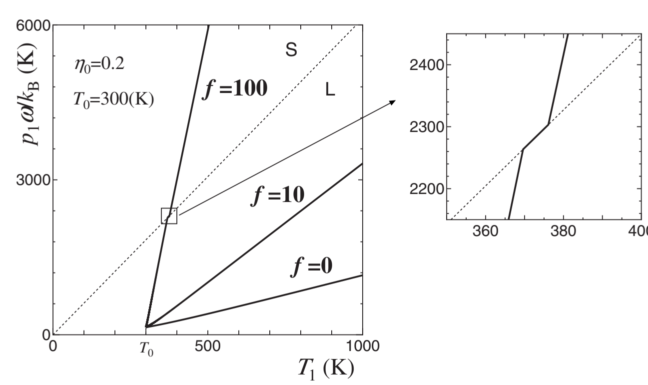

FIG. 3. Hugoniot loci, represented in the $p_1\omega/k_B$-T_1 plane for three different values of the internal degrees of freedom f $(f=0,10,100)$. In the case $f=100$, the Hugoniot loci cross the coexistence line, going from the liquid phase region to the solid phase region, as the shock strength increases (case P-2). The unperturbed packing fraction and temperature are given, respectively, by $\eta_0=0.2$ and $T_0=300$ K.

$$c_0 = \sqrt{\frac{k_B T_0}{m}\left(\Gamma_0 + \frac{2}{\mathcal{D}}\Gamma_0^2 + \eta_0\Gamma_0'\right)},$$

where Γ_i and Γ_i' $(i=0,1)$ are defined by

$$\Gamma_i \equiv \Gamma(\eta_i), \quad \Gamma_i' \equiv \left(\frac{d\Gamma(\eta)}{d\eta}\right)_{\eta_i}.$$

Without loss of generality, we hereafter assume for the Galilean invariance that $v_0=0$ and we will focus on the fastest shock wave propagating in the positive x direction.

We summarize in the following how the RH conditions appear after introducing the equations of state, Eqs. (1) and (3), into Eq. (7) (the details are essentially the same as in paper I) and we discuss some related subjects. Throughout the present paper, we study only the case in which the unperturbed states are in the region of liquid phase (i.e., $\eta_0 < \eta_L$).

A. Liquid-liquid and liquid-solid RH conditions

Since the equations of state for both liquid and solid phases have the same form [see Eqs. (1) and (3)], although the expressions of the function $\chi(\eta)$ are different, we write down the RH conditions in a unified way. The ratios of the pressure and temperature in the perturbed and unperturbed states, and the velocity in the perturbed state divided by the unperturbed sound velocity c_0, are given by

$$\hat{p} \equiv \frac{p_1}{p_0} = 1 + \frac{M_0^2(\hat{\eta}-1)[\Gamma_0(\mathcal{D}+2\Gamma_0)+\mathcal{D}\Gamma_0'\eta_0]}{\mathcal{D}\Gamma_0\hat{\eta}},$$

$$\hat{T} \equiv \frac{T_1}{T_0} = \frac{\hat{p}\Gamma_0}{\hat{\eta}\Gamma_1},$$

$$\hat{v} \equiv \frac{v_1}{c_0} = M_0\left(1-\frac{1}{\hat{\eta}}\right), \tag{8}$$

where $\hat{\eta} \equiv \eta_1/\eta_0$ and M_0 is expressed as

$$M_0 = \sqrt{\frac{\mathcal{D}\hat{\eta}\{-\mathcal{D}\Gamma_0+\Gamma_1[\mathcal{D}\hat{\eta}+2(\hat{\eta}-1)\Gamma_0]\}}{(\hat{\eta}-1)[\Gamma_1(1-\hat{\eta})+\mathcal{D}](\mathcal{D}\Gamma_0+2\Gamma_0^2+\mathcal{D}\eta_0\Gamma_0')}}. \tag{9}$$

Since we will be focusing on the fastest wave traveling in the positive x direction, we define a dimensionless characteristic velocity $\hat{\lambda}$ as follows:

$$\hat{\lambda} \equiv \frac{\lambda_3}{c_0} = \hat{v} + \sqrt{\frac{\hat{T}\left(\Gamma_1+\frac{2}{\mathcal{D}}\Gamma_1^2+\eta_1\Gamma_1'\right)}{\Gamma_0+\frac{2}{\mathcal{D}}\Gamma_0^2+\eta_0\Gamma_0'}}.$$

Note that, in all the above expressions,

$$\Gamma_0 \equiv \Gamma^L(\eta_0), \quad \Gamma_0' \equiv \left(\frac{d\Gamma^L(\eta)}{d\eta}\right)_{\eta_0},$$

and

$$\Gamma_1 \equiv \begin{cases} \Gamma^L(\eta_1), & \text{for } \eta_1 \text{ on the liquid branch; } L \text{ and } ML\text{—liquid-liquid RH conditions,} \\ \Gamma^S(\eta_1), & \text{for } \eta_1 \text{ on the solid branch; } S \text{ and } MS\text{—liquid-solid RH conditions,} \end{cases}$$

$$\Gamma_1' \equiv \begin{cases} \left(\frac{d\Gamma^L(\eta)}{d\eta}\right)_{\eta_1}, & \text{for } \eta_1 \text{ on the liquid branch; } L \text{ and } ML\text{—liquid-liquid RH conditions,} \\ \left(\frac{d\Gamma^S(\eta)}{d\eta}\right)_{\eta_1}, & \text{for } \eta_1 \text{ on the solid branch; } S \text{ and } MS\text{—liquid-solid RH conditions.} \end{cases}$$

B. Liquid-coexistence Rankine-Hugoniot conditions

We summarize the RH conditions in the case in which the perturbed state is a coexistence state (L-CO RH conditions). The total packing fraction $\eta(\alpha)$ of a coexistence state is given by

$$\frac{1}{\eta(\alpha)} = \frac{1-\alpha}{\eta_L} + \frac{\alpha}{\eta_S},$$

with the parameter α running from 0 to 1 as the coexistence state moves from the freezing point to the melting point on the horizontal line in Fig. 1. The pressure p^* is common to both phases and it is related to a common temperature T^* as follows:

$$\frac{p^*\omega}{k_B} = T^*\eta_L[1+\chi^L(\eta_L)] = T^*\eta_S[1+\chi^S(\eta_S)].$$

The following relations are obtained:

$$\hat{p} = 1 + \frac{M_0^2[\hat{\eta}(\alpha) - 1][\Gamma_0(\mathcal{D} + 2\Gamma_0) + \mathcal{D}\Gamma_0'\eta_0]}{\mathcal{D}\Gamma_0\hat{\eta}(\alpha)},$$

$$\hat{T} = \frac{\eta_0\{\Gamma_0\hat{\eta}(\alpha) + M_0^2(\Gamma_0 + 2\Gamma_0^2/\mathcal{D} + \eta_0\Gamma_0')[\hat{\eta}(\alpha) - 1]\}}{\Gamma^L(\eta_L)\eta_L\hat{\eta}(\alpha)},$$

$$\hat{v} = M_0\left(1 - \frac{1}{\hat{\eta}(\alpha)}\right),$$

$$M_0 = \sqrt{\frac{\dfrac{\mathcal{D}\hat{\eta}(\alpha)^2[\Gamma^L(\eta_L)\eta_L - \Gamma_0\eta_0]}{\hat{\eta}(\alpha) - 1} + 2\Gamma_0\hat{\eta}(\alpha)\Gamma^L(\eta_L)\eta_L}{(\Gamma_0 + 2\Gamma_0^2/\mathcal{D} + \eta_0\Gamma_0')\{\Gamma^L(\eta_L)\eta_L[1 - \hat{\eta}(\alpha)] + \mathcal{D}\eta_0\hat{\eta}(\alpha)\}}},$$

$$\hat{\lambda} = \hat{v} + \sqrt{\frac{\dfrac{2}{\mathcal{D}}\hat{T}[\Gamma^L(\eta_L)\eta_L]^2}{\hat{\eta}^2(\alpha)\eta_0^2\left(\Gamma_0 + \dfrac{2}{\mathcal{D}}\Gamma_0^2 + \eta_0\Gamma_0'\right)}}.$$

C. Two possibilities of shock-induced phase transitions

In paper I, the *Hugoniot loci* for the unperturbed states $\mathbf{u}_0$, $\mathcal{H}(\mathbf{u}_0)$, i.e., the loci of the perturbed states satisfying the RH conditions for a given unperturbed state $\mathbf{u}_0$ (also known as *RH curves*), in the two possible cases P-1 and P-2 of shock-induced phase transitions were analyzed in detail. Case P-1 is the phase transition with a jump between a metastable liquid state and a stable solid state, and case P-2 is the phase transition through coexistence states when the shock strength changes. We concluded that case P-2 is to be chosen, instead of case P-1, by adopting the selection rule in terms of the maximum entropy production rate: *the relevant case, from a physical point of view, is the one that involves the largest specific entropy production rate at a shock front as a function of the unperturbed Mach number.*

Therefore, it is an interesting problem to study whether the conclusion drawn in paper I is still true for a hard-sphere system with internal motion. We will study this problem in the next section and will conclude that case P-2 is still to be chosen for any value of the internal degrees of freedom f.

Before applying the selection rule to cases P-1 and P-2 (Sec. IV), we summarize the relations concerning the specific entropy production rate ς,

$$\varsigma = \eta_0 c_0 M_0 [\![s]\!],$$

where the jump of the specific entropy $[\![s]\!]$ for liquid-liquid, liquid-solid, and L-CO Hugoniot is given, respectively, by

$$[\![s]\!]^{L-L} = \frac{k_B}{m}\left(\frac{\mathcal{D}}{2}\ln\hat{T} - \int_{\eta_0}^{\eta_1}\frac{\Gamma^L(\eta)}{\eta}d\eta\right),$$

$$[\![s]\!]^{L-S} = \frac{k_B}{m}\left[\frac{\mathcal{D}}{2}\ln\hat{T} - \left(\int_{\eta_0}^{\eta_L}\frac{\Gamma^L(\eta)}{\eta}d\eta + \int_{\eta_S}^{\eta_1}\frac{\Gamma^S(\eta)}{\eta}d\eta\right) + \chi^S(\eta_S) - \chi^L(\eta_L)\right],$$

$$[\![s]\!]^{L-CO} = \frac{k_B}{m}\left(\frac{\mathcal{D}}{2}\ln\hat{T} - \int_{\eta_0}^{\eta_L}\frac{\Gamma^L(\eta)}{\eta}d\eta + \alpha[\chi^S(\eta_S) - \chi^L(\eta_L)]\right).$$

For details of these derivation, see paper I.

As a typical example, the dependence of the Hugoniot loci, $\mathcal{H}(\mathbf{u}_0)$, on the internal degrees of freedom, f, in case P-2 with the unperturbed state $\eta_0 = 0.2$ is shown in Figs. 2 and 3. For the sake of brevity, the Hugoniot loci in case P-1 are omitted. Noticeable points are summarized as follows:

(i) As the strength of a shock wave increases (that is, as η_1 increases from η_0), the quantities $\hat{p}$ and $\hat{T}$ increase, but their increasing rates decrease with the increase in the internal degrees of freedom, f. Moreover, the decrease in the increasing rate of $\hat{T}$ is larger than that of $\hat{p}$.

(ii) From Eqs. (8) and (9), it may be seen that the RH conditions have real solutions only when the denominator of the right-hand side of Eq. (9) is positive, i.e., when $\eta_0 \le \eta_1 < \eta_1^\infty$, with η_1^∞ being the perturbed packing fraction satisfying the relation

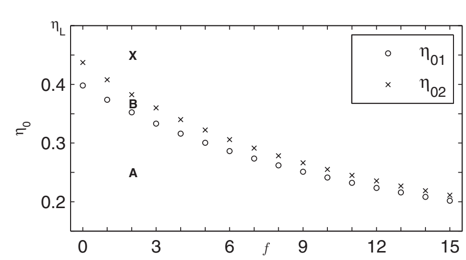

FIG. 4. Dependence of the characteristic packing fractions η_{01} and η_{02} on the internal degrees of freedom f. For each given value of f there are three distinct regions: A, B, and X.

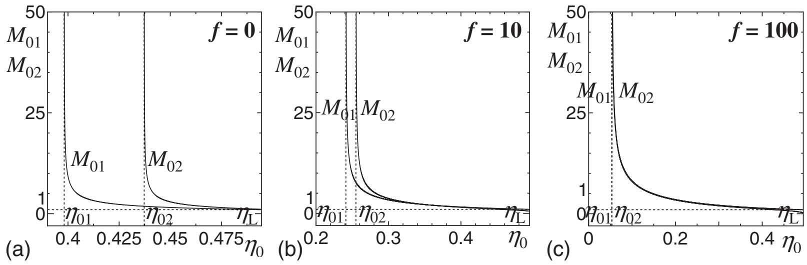

FIG. 5. Characteristic Mach numbers M_{01} and M_{02} versus the unperturbed packing fraction η_0 for several values of the internal degrees of freedom: $f=0$ (left), $f=10$ (center), and $f=100$ (right).

$$\Gamma(\eta_1^\infty)(1-\eta_1^\infty/\eta_0)+\mathcal{D}=0.$$

When η_1 tends to η_1^∞, $\hat{p}$ and $\hat{T}$, along with M_0, have a vertical asymptote (see Fig. 2); for this reason we call η_1^∞ the *strong shock limit*. It may be proved that η_1^∞ increases with the increase in the internal degrees of freedom, f.

(iii) From a physical point of view, we can understand that a considerable portion of the energy supplied by a shock compression goes into the internal motions of the system, and therefore the temperature cannot rise so much. This fact indicates that a shock-induced phase transition has a high possibility to take place in a hard-sphere system with large degrees of internal motion. In the figures, we can indeed observe a shock-induced phase transition when $f=100$.

D. Characteristic quantities

In paper I, some quantities useful in the classification of shock wave phenomena were introduced. Since those quantities will be useful in the following, we recall their definitions in this section.

The quantity η_{01} (η_{02}) is defined as the unperturbed packing fraction that leads to a perturbed packing fraction equal to η_L (η_S) in the strong shock limit. In other words, η_{01} (η_{02}) is the largest unperturbed packing fraction for which the liquid-coexistence (liquid-solid) shock-induced phase transition never occurs, no matter how the shock is strong.

These characteristic packing fractions, η_{01} and η_{02}, may be expressed as follows:

$$\eta_{01}=\eta_L\frac{\Gamma^L(\eta_L)}{\mathcal{D}+\Gamma^L(\eta_L)},\quad \eta_{02}=\eta_S\frac{\Gamma^S(\eta_S)}{\mathcal{D}+\Gamma^S(\eta_S)}. \tag{10}$$

It is easily seen from Eqs. (10) and (2) that η_{01} and η_{02} are decreasing (approaching zero) as f increases. This behavior is in agreement with the above-mentioned fact that the larger is f, the easier to obtain are the shock-induced phase transitions. As a consequence of the given definitions of η_{01} and η_{02}, we may define three distinct regions—graphically represented in Fig. 4—over which the unperturbed packing fraction η_0 can vary: region $\mathrm{A}=\{(f,\eta_0):f\in\mathbb{N},0<\eta_0<\eta_{01}\}$, region $\mathrm{B}=\{(f,\eta_0):f\in\mathbb{N},\eta_{01}<\eta_0<\eta_{02}\}$, and region $\mathrm{X}=\{(f,\eta_0):f\in\mathbb{N},\eta_{02}<\eta_0<\eta_L\}$. The dependence of η_{01} and η_{02} on the internal degrees of freedom, f, and the consequent effect of changing f on the extension of these three regions, may be appreciated in Fig. 4. A description of these three regions may be given as follows:

(1) Region A. When the unperturbed packing fraction η_0 is in this region, the perturbed states on the Hugoniot locus never have a packing fraction equal or larger to the packing fraction of the freezing point, η_L, even in the strong shock limit (i.e., $\eta_1^\infty<\eta_L$). Therefore, only a thermodynamically stable liquid state can be observed after a shock front, that is, shock-induced phase transition never occurs.

(2) Region B. When the unperturbed packing fraction η_0 is in this region, the perturbed states on the Hugoniot locus never have a packing fraction equal or larger than the packing fraction of the melting point, η_S, even thought it can be larger than the packing fraction of the freezing point, η_L (in other words, $\eta_L<\eta_1^\infty<\eta_S$). If the shock strength is large enough, we can observe a coexistence state after a shock front.

(3) Region X. When the unperturbed packing fraction η_0 is in this region, the perturbed states on the Hugoniot locus may have a packing fraction larger than the packing fraction of the melting point, η_S (i.e., $\eta_1^\infty>\eta_S$). Therefore, if the shock strength is large enough, we can observe a stable solid state after a shock front. There can exist shock-induced liquid-solid phase transitions.

Other quantities, already introduced in paper I, that turn out to be useful in the present analysis are the following. The quantity M_{01} (M_{02}) is defined as the unperturbed Mach number that leads to a perturbed state with a packing fraction equal to η_L (η_S). In other words, M_{01} (M_{02}) is the smallest unperturbed Mach number for which a liquid-coexistence (liquid-solid) shock-induced phase transition occurs, if ever.

The characteristic Mach numbers M_{01} and M_{02} may be expressed as follows:

$$M_{01}=\sqrt{\frac{\mathcal{D}\hat{\eta}_L\{-\mathcal{D}\Gamma_0+\Gamma^L(\eta_L)[\mathcal{D}\hat{\eta}_L+2(\hat{\eta}_L-1)\Gamma_0]\}}{(\hat{\eta}_L-1)[\Gamma^L(\eta_L)(1-\hat{\eta}_L)+\mathcal{D}](\mathcal{D}\Gamma_0+2\Gamma_0^2+\mathcal{D}\eta_0\Gamma_0')}},$$

$$M_{02}=\sqrt{\frac{\mathcal{D}\hat{\eta}_S\{-\mathcal{D}\Gamma_0+\Gamma^S(\eta_S)[\mathcal{D}\hat{\eta}_S+2(\hat{\eta}_S-1)\Gamma_0]\}}{(\hat{\eta}_S-1)[\Gamma^S(\eta_S)(1-\hat{\eta}_S)+\mathcal{D}](\mathcal{D}\Gamma_0+2\Gamma_0^2+\mathcal{D}\eta_0\Gamma_0')}}.$$

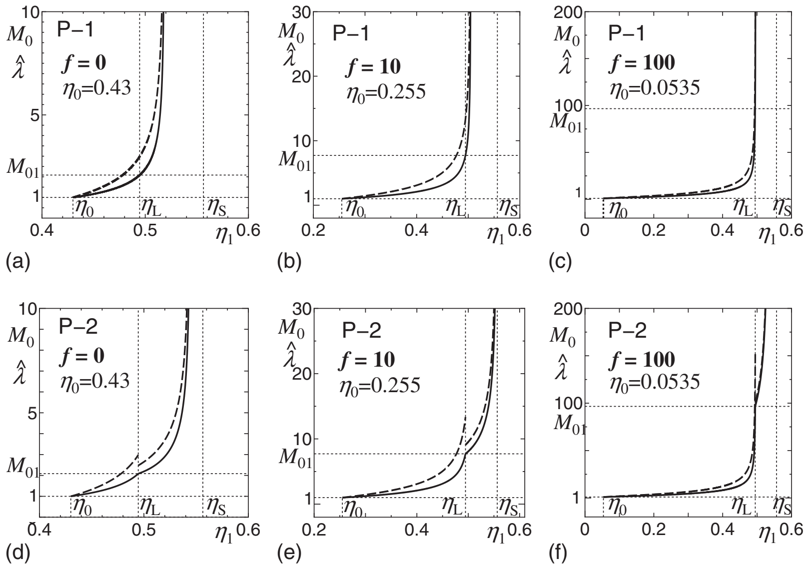

FIG. 6. Dependences of the unperturbed Mach number M_0 (solid curve) and of the dimensionless characteristic speed $\hat{\lambda}$ (dashed curve) on the perturbed packing fraction η_1 for three different values of the internal degrees of freedom f ($f=0,10,100$) according to the possibilities P-1 (above) and P-2 (below). The unperturbed packing fraction η_0 is in region B.

The dependence of M_{01} and M_{02} on the internal degrees of freedom, f, is shown in Fig. 5.

IV. ADMISSIBILITY OF SHOCK WAVES

From the theory of hyperbolic systems, it is well known that some conditions (a selection rule) have to be satisfied in order for a shock to be allowed to propagate. Such a shock satisfying the proper selection rule will be referred to as an *admissible* shock. Since an admissible shock is a shock that does not change its wave profile during its propagation, while the wave profile of an inadmissible shock breaks into a combination of shocks, rarefaction waves and constant states evolving in time, an admissible shock is sometimes called a *stable* shock in the literature concerning hyperbolic system.

In the case of a genuinely nonlinear field, i.e., if the following condition is satisfied:

$$\nabla\lambda \cdot \mathbf{r} \neq 0 \quad \forall \quad \mathbf{u},$$

where λ is an eigenvalue of the hyperbolic systems, ∇ is the gradient made with respect to $\mathbf{u}$, and $\mathbf{r}$ is the corresponding eigenvector, the selection rule is given by the well-known Lax conditions [43], stating that a shock is admissible if its velocity of propagation, U_s, is such that

$$\lambda_0 < U_s < \lambda_1,$$

with λ_0 and λ_1 being, respectively, the eigenvalues evaluated in the unperturbed and perturbed states. In the case of a locally genuinely nonlinear field, i.e., when the genuine nonlinearity fails for some values of the field,

$$\nabla\lambda \cdot \mathbf{r} = 0 \quad \text{for some} \quad \mathbf{u},$$

the Lax conditions have to be replaced with the more general Liu conditions [44–46] asserting that a shock is admissible if and only if its velocity of propagation is not decreasing as we move on the Hugoniot locus starting from the unperturbed state $\mathbf{u}_0$ toward the given perturbed state $\mathbf{u}_1$,

$$U_s(\mathbf{u}_0,\tilde{\mathbf{u}}) \leq U_s(\mathbf{u}_0,\mathbf{u}_1) \quad \forall \quad \tilde{\mathbf{u}} \in \mathcal{H}(\mathbf{u}_0) \text{ between } \mathbf{u}_0 \text{ and } \mathbf{u}_1.$$

First of all, let us consider two typical cases. In the first case (Figs. 6 and 7) the unperturbed packing fraction η_0 is in region B (see Fig. 4); in the second case (Figs. 8 and 9) the unperturbed packing fraction η_0 lies in region X. From Figs. 6 and 8, we see that in both the two cases, both possibilities P-1 and P-2 guarantee that the Liu conditions are satisfied. From Figs. 7 and 9, we can see that both possibilities P-1 and P-2 satisfy also the thermodynamical requirement of the positivity of the entropy production rate ς in both the two cases. Therefore, shock waves of both possibilities P-1 and P-2 are stable.

The problem to be solved now consists of understanding which of the two possibilities is the physically relevant one. It can be proved that the entropy production rate ς of possibility P-2 is larger than that of possibility P-1 for any value of the internal degrees of freedom, f, although the difference between possibilities P-1 and P-2 decreases with the increase in f. Here, for the sake of brevity, we omit the proof. Therefore, if we use the selection rule in terms of the maximum

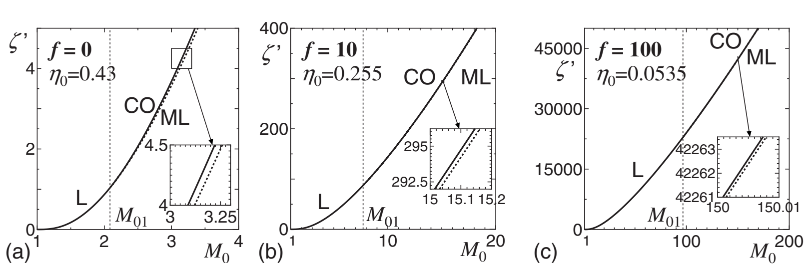

FIG. 7. Dependence of the dimensionless entropy production rate ς' [$=(\varsigma/\eta_0 c_0)(m/k_B)$] on the unperturbed Mach number M_0 for three different values of the internal degrees of freedom f ($f=0,10,100$) according to the possibilities P-1 (dotted curve) and P-2 (solid curve). The unperturbed packing fraction η_0 is in region B.

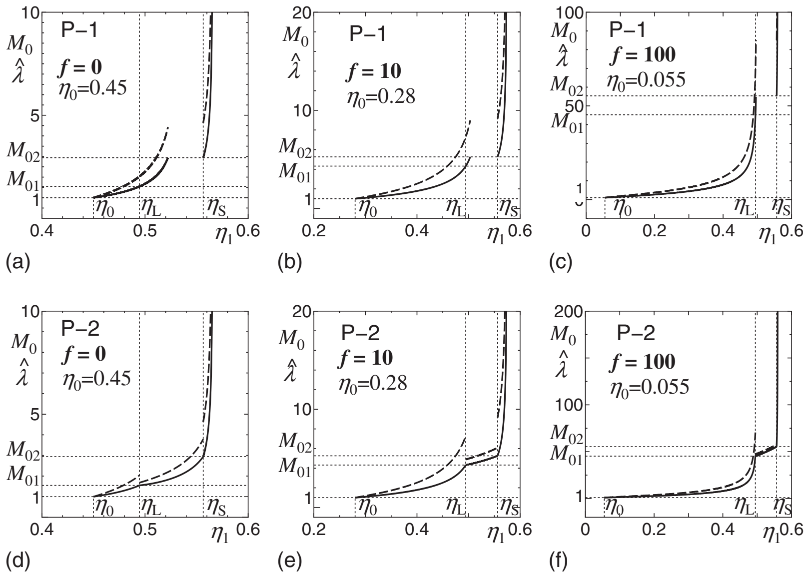

FIG. 8. Dependences of the unperturbed Mach number M_0 (solid curve) and of the dimensionless characteristic speed $\hat{\lambda}$ (dashed curve) on the perturbed packing fraction η_1 for three different values of the internal degrees of freedom f ($f=0,10,100$) according to the possibilities P-1 (above) and P-2 (below). The unperturbed packing fraction η_0 is in region X.

entropy production rate mentioned in the last section, we may adopt the coexistence Hugoniot (possibility P-2) as the physically relevant solution for a hard-sphere system with internal motion. According to this, hereafter, we will confine our analysis to the study of only possibility P-2.

V. CLASSIFICATION OF SHOCK-INDUCED LIQUID-SOLID PHASE TRANSITIONS

In Sec. III D, we stated that, for any given f, a shock-induced liquid-solid phase transition may occur only when the unperturbed packing fraction lies in region X (see Fig. 4). In this section, we study the fine structure of this region: we divide it into three subregions and we motivate this subdivision pointing out the different features of these three subregions in terms of shock admissibility. Let us pay attention to the following three cases, covering all the possible relations between the unperturbed Mach number M_0 and the perturbed packing fraction η_1 in region X:

(i) The unperturbed Mach number M_0 is a monotonically increasing function of the perturbed packing fraction η_1. Therefore, the characteristic Mach numbers M_{01} and M_{02} satisfy the inequality $M_{01}<M_{02}$ [cf. case (α) in Fig. 10].

(ii) The unperturbed Mach number M_0 is not a monotonically increasing function of the perturbed packing fraction η_1, and there is a packing fraction η_c ($\eta_L<\eta_c<\eta_S$) such that $M_0=M_{01}$ when $\eta_1=\eta_c$. The inequality $M_{01}<M_{02}$ still holds in this case [cf. case (β) in Fig. 10].

(iii) The unperturbed Mach number M_0 is not a monotonically increasing function of the perturbed packing fraction η_1, as in case (ii), but the packing fraction η_c satisfies, in this case, the inequality $\eta_c>\eta_S$. The inequality $M_{01}>M_{02}$ holds in this case [cf. cases (γ) and (δ) in Fig. 10].

We can prove that the boundary between cases (i) and (ii) is characterized by the condition that the characteristic unperturbed Mach number M_{01} is equal to the characteristic speed estimated by using the L-CO Hugoniot conditions $\hat{\lambda}^{CO}$ at the freezing point η_L,

$$M_{01}=\hat{\lambda}^{CO}|_{\eta_L}. \tag{11}$$

The boundary between cases (ii) and (iii) is given by the condition

$$M_{01}=M_{02}. \tag{12}$$

By using conditions (11) and (12) we realize that region X may be divided into three distinct subregions C, D, and Y, which correspond to cases (i), (ii), and (iii), respectively, as shown in Fig. 11. In fact, for any $f>0$, there exists an unperturbed packing fraction η_{03}, for which condition (11) is satisfied and, analogously, there exists an unperturbed packing fraction η_{04}, for which condition (12) is satisfied; all the unperturbed packing fractions such that $\eta_{02}<\eta_0<\eta_{03}$ belong to case (i), all the ones such that $\eta_{03}<\eta_0<\eta_{04}$ belong to case (ii), and all those such that $\eta_{04}<\eta_0<\eta_L$ belong to case (iii). When $f=0$, it turns out that condition (12) is never

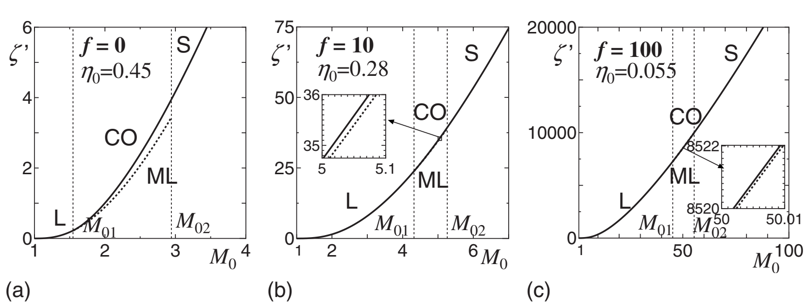

FIG. 9. Dependence of the dimensionless entropy production rate ς' [$=(\varsigma/\eta_0 c_0)(m/k_B)$] on the unperturbed Mach number M_0 for three different values of the internal degrees of freedom f ($f=0,10,100$) according to the possibilities P-1 (dotted curve) and P-2 (solid curve). The unperturbed packing fraction η_0 is in region X.

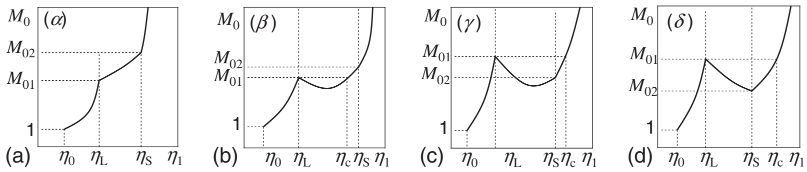

FIG. 10. Schematic representations of typical cases of the relationship between the unperturbed Mach number M_0 and the perturbed packing fraction η_1 in region X.

satisfied; in this case any unperturbed packing fractions such that $\eta_{03} < \eta_0 < \eta_L$ belong to case (ii). So, region $C = \{(f, \eta_0) : f \in \mathbb{N}, \eta_{02} < \eta_0 < \eta_{03}\}$, region $D = \{(f, \eta_0) : f \in \mathbb{N}_+, \eta_{03} < \eta_0 < \eta_{04}\} \cup \{(f, \eta_0) : f = 0, \eta_{03} < \eta_0 < \eta_L\}$, and region $Y = \{(f, \eta_0) : f \in \mathbb{N}_+, \eta_{04} < \eta_0 < \eta_L\}$.

We summarize in the following the characteristic features of regions C, D, and Y in detail by studying the case $f = 10$, pointing out that the results are qualitatively valid for any $f > 0$:

(1) Region C. The dependence of the unperturbed Mach number M_0 and of the dimensionless characteristic speed $\hat{\lambda}$ on the perturbed packing fraction η_1 in a typical case ($\eta_0 = 0.28$) is shown in Fig. 12. We notice that, from the Liu conditions, any compressive shock wave ($\eta_1 > \eta_0$) is admissible. In other words, by using a single compressive shock, we can obtain any stable perturbed state in any phase (liquid phase, coexistence, and solid phase). The same property of the admissibility for a single shock was already found in the case of $f = 0$ presented in paper I.

(2) Region D. The dependence of the unperturbed Mach number M_0 and of the dimensionless characteristic speed $\hat{\lambda}$ on the perturbed packing fraction η_1 in the case with $\eta_0 = 0.35$ is shown in Fig. 13. The intersection point between M_0 and $\hat{\lambda}$ in the coexistence region is the local minimum point of M_0. A noticeable point is that, from the Liu conditions, a shock wave with a perturbed packing fraction such that $\eta_0 < \eta_1 < \eta_L$ and $\eta_1 > \eta_c$ is admissible, while a shock wave with a perturbed packing fraction such that $\eta_L < \eta_1 < \eta_c$ is not admissible. That is to say, it is impossible to reach a perturbed state with the packing fraction in the part of the coexistence region $\eta_L < \eta_1 < \eta_c$ through a stable shock. In the next section we will study the stability of a shock wave numerically and will confirm the above results.

If an initial shock is in the above-mentioned inadmissible region, such a shock eventually splits into several waves composed of shock waves, rarefaction waves, and constant states in the course of its propagation. Some typical numerical examples of the shock splitting and composite waves occurred thereby will be shown also in the next section. Shock splitting phenomena in a gas [47–49] and in a solid [28] have already been studied.

(3) Region Y. Let us discuss region Y that is characteristic of a hard-sphere system with internal degrees of freedom $f \geq 1$. Typical dependence of the Mach number M_0 and the dimensionless characteristic speed $\hat{\lambda}$ on the packing fraction η_1 is shown in Figs. 14 and 15 [see cases (γ) and (δ) in Fig. 10]. The unperturbed Mach number M_0 has a local minimum point in the coexistence region (see Fig. 14) or it is monotonically decreasing, as η_1 increases, all over the coexistence region (see Fig. 15). As far as a stable single shock is concerned, we can study both cases simultaneously.

From the Liu conditions, a shock wave with a perturbed state in the region $\eta_0 < \eta_1 < \eta_L$ and $\eta_1 > \eta_c$ is admissible, while a shock wave with a perturbed state in the region $\eta_L < \eta_1 < \eta_c$ is not admissible. As in region D, it is impossible to reach a perturbed state with the packing fraction in the region $\eta_L < \eta_1 < \eta_c$ through a single stable shock. However, it should be noticed that the unstable region in this case includes the melting point η_S and therefore includes a part of the Hugoniot locus in thermodynamically stable solid phase. Therefore, a shock wave may be unstable even though the perturbed state is in thermodynamically stable solid phase. This is one of the remarkable features of the dynamic phase transitions found in the present analysis. In material syntheses, for example, this fact may become important because we have now noticed that there are thermodynamic stable states which cannot be reached by a single shock. In the next section we will study numerically the stability of a shock wave and the shock splitting.

VI. NUMERICAL ANALYSIS

In the previous sections, we have used the Liu conditions in our analysis. Rigorously speaking, the Liu conditions require the constitutive equations to be smooth, so they are not applicable when the Hugoniot loci cross neighborhoods of perturbed states with packing fractions equal to η_L or η_S, because the equations of state are not smooth when $\eta = \eta_L$ and $\eta = \eta_S$. In these cases, the numerical approach plays a major role showing that the results concerning the shock admissibility are the same as if the Liu conditions were applicable.

Numerical solutions of the equations for the hard-sphere system described in Sec. II have been calculated in order to check the theoretical results stated in Sec. V and to analyze the admissibility of a shock wave when its unperturbed state lies in one of the regions labeled as A, B, C, D, and Y. The tool used for the computations is a MATLAB/C++ general-purpose code useful for the numerical solution of hyperbolic

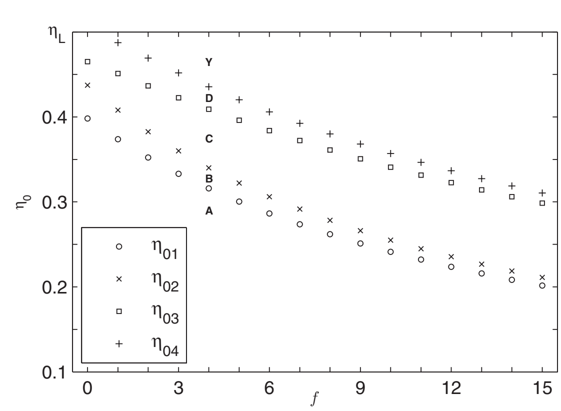

FIG. 11. Region X may be divided into the three subregions C, D, and Y.

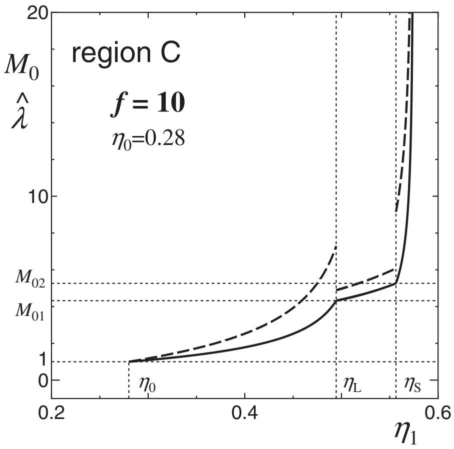

FIG. 12. Typical dependences of the Mach number M_0 (solid curve) and of the dimensionless characteristic speed $\hat{\lambda}$ (broken curve) on the perturbed packing fraction η_1. Any shock wave with a perturbed state ($\eta_1 > \eta_0$) is stable.

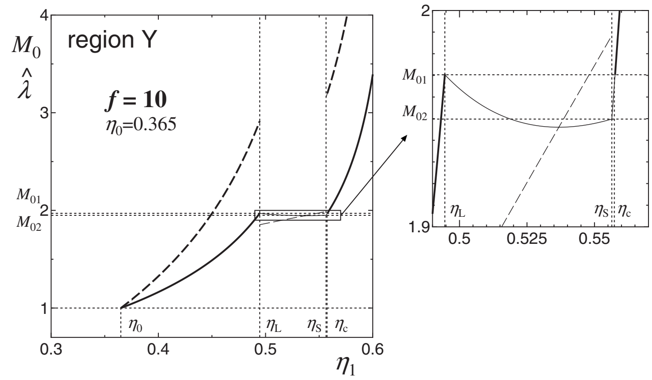

FIG. 14. Typical dependences of the Mach number M_0 (solid curve) and of the dimensionless characteristic speed $\hat{\lambda}$ (broken curve) on the perturbed packing fraction η_1. A shock wave with the perturbed packing fraction η_1 in the region $\eta_0 < \eta_1 < \eta_L$ and $\eta_1 > \eta_c$ is stable (boldfaced part of the curve M_0), while a shock wave with a perturbed packing fraction η_1 such that $\eta_L < \eta_1 < \eta_c$ is unstable (lightfaced part of the curve M_0). The unstable region includes the melting point η_S.

systems of balance and/or conservation laws, which has been recently developed by some of the authors [50,51]. The tool allows the user to choose the suitable algorithm among a wide variety of available algorithms. For this case, the selected algorithm is based on a fourth-order central Runge-Kutta scheme recently proposed by Pareschi *et al.* [52], which turned out to be stable and sound for a wide range of hyperbolic systems of conservation laws, including the case of locally linearly degenerate fields.

When the unperturbed state $\mathbf{u}_0$ belongs to one of regions A, B, and C, the Liu conditions give the same results as the Lax conditions and it turns out that all the states $\mathbf{u}_1$ lying on the admissible branch of the Hugoniot locus passing through the given state $\mathbf{u}_0$ are connected to $\mathbf{u}_0$ by an admissible shock wave, i.e., all the compressive shocks are admissible. This well-known theoretical result has been checked by means of numerical calculations and some representative results are shown in Fig. 16 for the cases of $\mathbf{u}_0$ belonging to regions A–C. For each of these three cases, given an unperturbed state $\mathbf{u}_0 \equiv (\eta_0, v_0, p_0\omega/m)$, we show the profile of η as a function of x at $t=0.2$ which comes from a Cauchy initial data of Riemann type in which the discontinuity between the unperturbed state $\mathbf{u}_0$ and the perturbed state $\mathbf{u}_1$ is located at $x=0$. The value of the internal degrees of freedom is set to $f=10$.

For case A, the packing fraction of the considered unperturbed state is $\eta_0=0.2$; for case B, the packing fraction is $\eta_0=0.255$ and, finally, for case C we set $\eta_0=0.28$. All the calculations have been performed with $v_0=0$ and $p_0\omega/m=0.3$. In all these cases the packing fractions of the perturbed states, η_1, for which numerical results are presented are graphically shown in Fig. 16 (left column) by means of black circles. From the corresponding η profiles, obtained numerically and given in Fig. 16 (right column), we may claim that the shock wave appears to be acceptable for any of the perturbed state that we have examined.

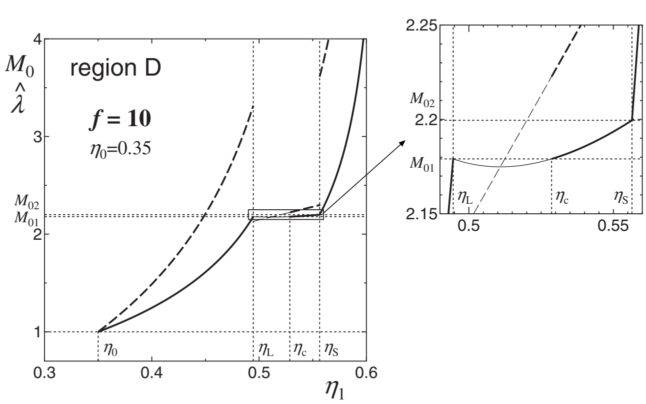

FIG. 13. Typical dependences of the Mach number M_0 (solid curve) and of the dimensionless characteristic speed $\hat{\lambda}$ (broken curve) on the perturbed packing fraction η_1. A shock wave with the perturbed packing fraction η_1 in the region $\eta_0 < \eta_1 < \eta_L$ and $\eta_1 > \eta_c$ is stable (boldfaced part of the curve M_0), while a shock wave with a perturbed packing fraction such that $\eta_L < \eta_1 < \eta_c$ is unstable (lightfaced part of the curve M_0).

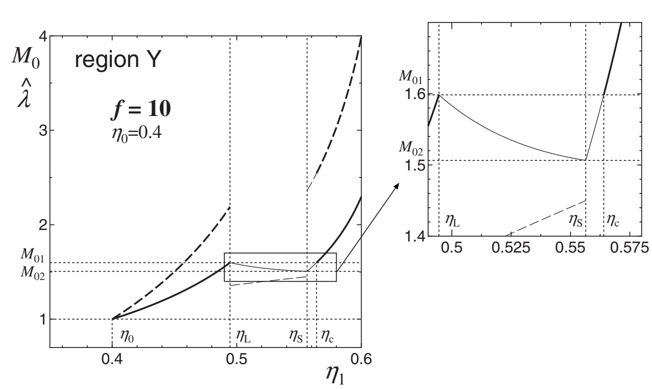

FIG. 15. Typical dependences of the Mach number M_0 (solid curve) and of the dimensionless characteristic speed $\hat{\lambda}$ (broken curve) on the perturbed packing fraction η_1. A shock wave with the perturbed packing fraction η_1 in the region $\eta_0 < \eta_1 < \eta_L$ and $\eta_1 > \eta_c$ is stable (boldfaced part of the curve M_0), while a shock wave with η_1 in the region $\eta_L < \eta_1 < \eta_c$ is unstable (lightfaced part of the curve M_0). The unstable region includes the melting point η_S.

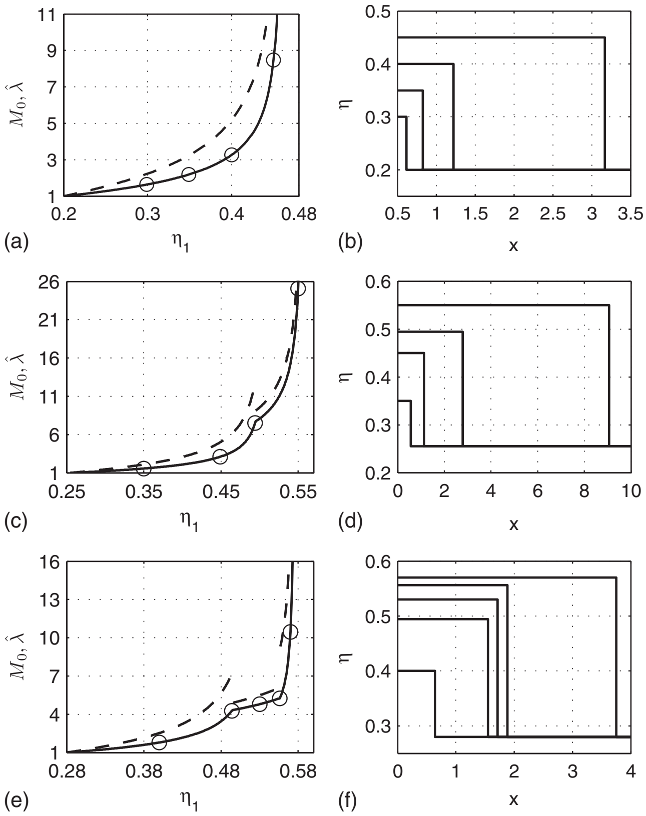

FIG. 16. Left column: M_0 and $\hat{\lambda}$ as functions of η_1 for unperturbed states defined by $v_0=0$, $p_0\omega/m=0.3$, and (from top to bottom) $\eta_0=0.2$ (region A), $\eta_0=0.255$ (region B), and $\eta_0=0.28$ (region C). Right column: η profiles obtained numerically as solutions of the Riemann problem with unperturbed states defined above and perturbed states indicated by the black circles in the left figures: (top) $\eta_1=0.3,0.35,0.4,0.45$; (middle) $\eta_1=0.35,0.45,0.4946,0.55$; and (bottom) $\eta_1=0.4,0.4946,0.53,0.5564,0.573$.

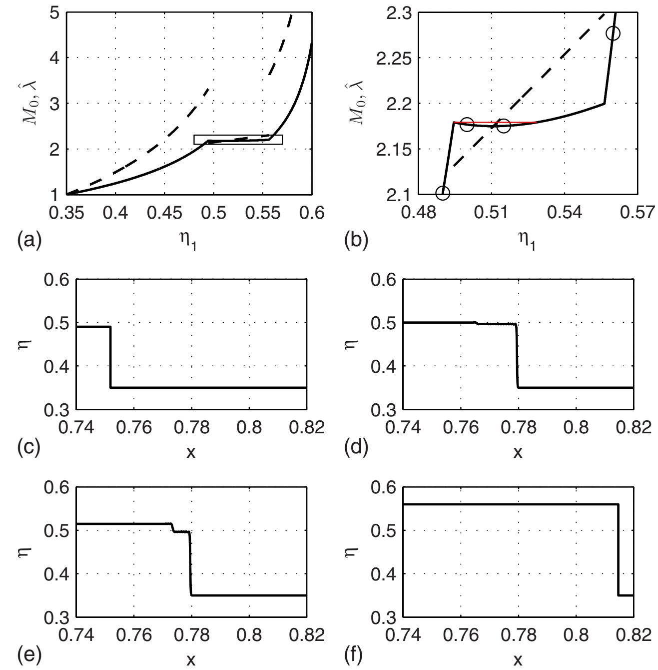

FIG. 17. (Color online) (Region D) Top row: (left) M_0 and $\hat{\lambda}$ as functions of η_1 for an unperturbed state defined by $\eta_0=0.35$, $v_0=0$, and $p_0\omega/m=0.3$; (right) blowup of the boxed region in the left side. Second and third rows: η profiles obtained numerically as solutions of the Riemann problem with unperturbed states defined above and perturbed states indicated by the black circles in the blowup: (from left to right, from top to bottom) $\eta_1=0.49,0.5,0.515,0.56$.

The numerical analysis of the admissibility of shock waves whose unperturbed state lies in region D is presented in Fig. 17 for $\eta_0=0.35$. In this case, the Lax conditions are not applicable and the Liu conditions become necessary in order to analyze the admissibility of shocks. The range of the η_1 values for which the Liu conditions allow to claim that the shock is not admissible corresponds to the region under the horizontal thin line in Fig. 17 (top right), that is, $\eta_L < \eta_1 < \eta_c$, while the values of η_1 outside this interval ($\eta_0 \leq \eta_1 \leq \eta_L$ and $\eta_1 \geq \eta_c$) give admissible shocks. The numerical solutions, presented here for a set of perturbed states whose packing fraction spans all the regions of interest, confirm the theoretical results, as may be appreciated from the profiles of the packing fraction η shown in Fig. 17 (second and third rows).

Numerical results concerning the case in which the unperturbed state $\mathbf{u}_0$ lies in region Y are presented in Fig. 18. In this case, as pointed out in Sec. V, a shock wave with a perturbed packing fraction η_1 in the solid branch ($\eta_1 > \eta_S$) may be not acceptable, as well as all the shock waves with packing fractions in the coexistence region ($\eta_L < \eta_1 < \eta_S$). In fact, from the Liu conditions, we obtain that a shock is admissible if $\eta_0 \leq \eta_1 \leq \eta_L$ or $\eta_1 \geq \eta_c > \eta_S$. This means that all the perturbed states lying on the Hugoniot locus through $\mathbf{u}_0$ such that $\eta_S < \eta_1 < \eta_c$ ($\eta_S \simeq 0.5564$, $\eta_c \simeq 0.5576$) are not acceptable. These results are confirmed by the numerical solutions, as may be appreciated from Fig. 18 (second and third rows). It is worth noting that, in the presented cases of nonadmissible shocks [i.e., the cases in Fig. 17 (middle right and bottom left) and in Fig. 18 (middle right and bottom left)], the η profiles show the so-called *shock splitting* phenomenon, i.e., the wave profile is made up with a combination of shock waves, rarefaction waves, and constant states, depending on the particular values of the unperturbed and perturbed states.

VII. SUMMARY AND CONCLUDING REMARKS

From the analysis of the RH conditions, we have found the distinct regions A, B, C, D, and Y in the plane of the unperturbed packing fraction η_0 and the internal degrees of freedom f (Fig. 11). It is interesting to note that region Y can be observed only if $f \geq 1$, that is, if there is an internal motion.

The characteristic features of regions A–C have already been discussed through studying the cases of no internal motion (i.e., $f=0$) in paper I. Regions D and Y are essentially unique findings in the present paper. By applying the Liu conditions to the cases in regions D and Y we have made clear the admissible condition for a stable single shock wave.

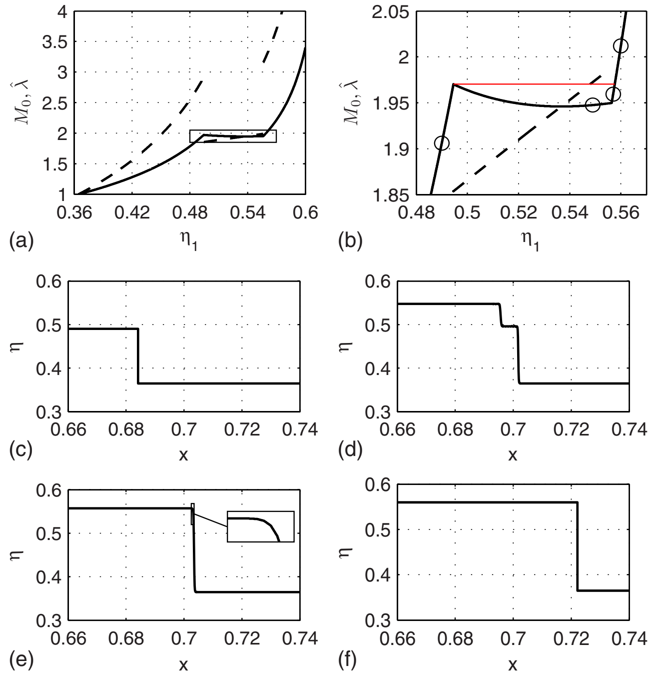

FIG. 18. (Color online) (Region Y) Top row: (left) M_0 and $\hat{\lambda}$ as functions of η_1 for an unperturbed state defined by $\eta_0=0.365$, $v_0=0$, and $p_0\omega/m=0.3$; (right) blowup of the boxed region in the left side. Second and third rows: η profiles obtained numerically as solutions of the Riemann problem with unperturbed state defined above and perturbed states indicated by the black circles in the blowup: (from left to right, from top to bottom) $\eta_1=0.49, 0.549, 0.557, 0.56$.

Even if a perturbed state is thermodynamically stable, it is not always stable dynamically, that is, it may be unstable with respect to a dynamical perturbation. In such an unstable case we can observe the so-called shock splitting phenomena as shown in the numerical analysis in Sec. VI.

Lastly let us summarize the concluding remarks as follows:

(i) In the present analysis, our study is mainly limited within analyzing stable shock waves. If we want to study the time evolution of an unstable single shock in detail, we should divide region Y into more subregions in order to classify such time evolutions properly [see, for example, cases (γ) and (δ) in Fig. 10 both of which belong to the same region Y]. The subject is left for a future work.

(ii) Here, we have studied only plane shock waves. Study of the other kinds of shock waves, for example, spherical shock waves seems to be interesting.

(iii) Only shock-induced phase transitions from liquid phase to solid phase can be observed in the present model. Inverse transition can never be observed. It should be emphasized that this does not mean that there are no phase transitions in a solid under shock compression [7,17,19,20,22,23,25–31].

(iv) By using all the results obtained in paper I and the present paper and by using the perturbation method developed in the theory of liquid-state physics [36–38], we can study physical systems with more realistic interatomic potential with both repulsive and attractive parts. In subsequent papers, we will study shock wave phenomena and shock-induced phase transitions by taking three phases (gas, liquid, and solid phases) into account in a unified way.

(v) Shock waves in a system of fullerenes C_{60} afford us with possible experiments to check the present theory. In fact, we can expect to observe shock-induced liquid-solid phase transitions in this kind of system. The experimental data can be compared with the present results of a suitable nonzero value of f. However, the success of such experiments is not so much sure at present because the liquid phase of the system has not been observed clearly until now [53–55].

(vi) A more general case, that is, nonpolytropic case where f is temperature dependent is the subject of a recent paper [56].

ACKNOWLEDGMENTS

The authors thank Professor H. Nakamura and Dr. A. Ito (National Institute for Fusion Science) for their valuable comments. This work was partially supported by Japan Society of Promotion of Science (JSPS) Grants No. 08J08281 (S.T.) and No. 20560054 (M.S.), National Group of Mathematical Physics GNFM-INdAM (A.M., Young Research Project 2009, and T.R.), Heiwa Nakajima Foundation 2009 (M.S. and N.Z.), and National Natural Science Foundation of China (NSFC) Grant No. 20973119 (N.Z.).

[1] G. B. Whitham, *Linear and Nonlinear Waves* (John Wiley and Sons, New York, 1974).
[2] C. Dafermos, *Hyperbolic Conservation Laws in Continuum Physics*, 3rd ed. (Springer Verlag, Berlin, 2010).
[3] I. Müller and T. Ruggeri, *Rational Extended Thermodynamics* (Springer-Verlag, New York, 1998).
[4] S. Chapman and T. G. Cowling, *The Mathematical Theory of Non-Uniform Gases* (Cambridge University Press, Cambridge, England, 1970).
[5] H. Struchtrup, *Macroscopic Transport Equations for Rarefied Gas Flows: Approximation Methods in Kinetic Theory* (Springer-Verlag, Berlin, 2005).
[6] L. D. Landau and E. M. Lifshitz, *Fluid Mechanics*, 2nd ed. (Pergamon Press, London, 1987).
[7] G. E. Duvall and R. A. Graham, Rev. Mod. Phys. **49**, 523 (1977).
[8] *High-Pressure Shock Compression of Solids*, edited by J. R. Asay and M. Shahinpoor (Springer-Verlag, New York, 1992).
[9] R. A. Graham, *Solids Under High-Pressure Shock Compression: Mechanics, Physics, and Chemistry* (Springer-Verlag, New York, 1992).
[10] *Shock Waves in Materials Science*, edited by A. B. Sawaoka

(Springer-Verlag, Tokyo, 1993).
[11] *High-Pressure Shock Compression of Solids II*, edited by L. Davison, D. Grandy, and M. Shahinpoor (Springer-Verlag, New York, 1996).
[12] *High-Pressure Shock Compression of Solids III*, edited by L. Davison and M. Shahinpoor (Springer-Verlag, New York, 1997).
[13] *High-Pressure Shock Compression of Solids IV*, edited by L. Davison, Y. Horie, and M. Shahinpoor (Springer-Verlag, New York, 1997).
[14] *High-Pressure Shock Compression of Solids V*, edited by L. Davison, Y. Horie, and T. Sekine (Springer-Verlag, New York, 2002).
[15] *High-Pressure Shock Compression of Solids VI*, edited by Y. Horie, L. Davison, and N. N. Thadhani (Springer-Verlag, New York, 2002).
[16] *High-Pressure Shock Compression of Solids VII*, edited by V. E. Fortov, L. V. Al'tshuler, R. F. Trunin, and A. I. Funtikov (Springer-Verlag, New York, 2003).
[17] D. G. Morris, J. Appl. Phys. **51**, 2059 (1980).
[18] A. Matsuda, K. Kondo, and K. G. Nakamura, J. Chem. Phys. **124**, 054501 (2006).
[19] C. S. Yoo, N. C. Holmes, M. Ross, D. J. Webb, and C. Pike, Phys. Rev. Lett. **70**, 3931 (1993).
[20] C. Dai, X. Jin, X. Zhou, J. Liu, and J. Hu, J. Phys. D: Appl. Phys. **34**, 3064 (2001).
[21] D. A. Boness, Ph.D. thesis, University of Washington, 1991.
[22] R. S. Hixson, D. A. Boness, J. W. Shaner, and J. A. Moriarty, Phys. Rev. Lett. **62**, 637 (1989).
[23] A. B. Belonoshko, Science **275**, 955 (1997).
[24] M. Woo and I. Greber, AIAA J. **37**, 215 (1999).
[25] J. W. Jeong, I. H. Lee, and K. J. Chang, Phys. Rev. B **59**, 329 (1999).
[26] J. W. Jeong and K. J. Chang, J. Phys.: Condens. Matter **11**, 3799 (1999).
[27] S. N. Luo, T. J. Ahrens, T. Çağin, A. Strachan, W. A. Goddard, and D. C. Swift, Phys. Rev. B **68**, 134206 (2003).
[28] K. Kadau, T. C. Germann, P. S. Lomdahl, and B. L. Holian, Science **296**, 1681 (2002).
[29] S. N. Luo and T. J. Ahrens, Phys. Earth Planet. Inter. **143-144**, 369 (2004).
[30] L. V. Al'tshuler, Zh. Prikl. Mekh. Tekh. Fiz. **4**, 93 (1978).
[31] M. Ross, Phys. Rev. A **8**, 1466 (1973).
[32] N. Zhao, M. Sugiyama, and T. Ruggeri, J. Chem. Phys. **129**, 054506 (2008).
[33] J. B. Alder and T. E. Wainwright, J. Chem. Phys. **27**, 1208 (1957).
[34] J. B. Alder and T. E. Wainwright, Phys. Rev. **127**, 359 (1962).
[35] W. G. Hoover and F. H. Ree, J. Chem. Phys. **49**, 3609 (1968).
[36] A. Münster, *Statistical Thermo-Dynamics* (Springer-Verlag, Berlin, 1974), Vol. 2.
[37] J. A. Barker and D. Henderson, Rev. Mod. Phys. **48**, 587 (1976).
[38] J. P. Hansen and J. R. McDonald, *Theory of Simple Liquids* (Academic Press, London, 1986).
[39] P. A. Thompson, G. A. Carofano, and Y. Kim, J. Fluid Mech. **166**, 57 (1986).
[40] G. E. A. Meier, in *Multiphase Flows I*, Shock Wave Science and Technology Reference Library Vol. 1, edited by M. E. H. van Dongen (Springer, Berlin, 2007), Chap. 7, pp. 231–267.
[41] N. Zhao, A. Mentrelli, T. Ruggeri, and M. Sugiyama (unpublished).
[42] L. V. Woodcock, J. Chem. Soc., Faraday Trans. 2 **72**, 731 (1976).
[43] P. D. Lax, Commun. Pure Appl. Math. **10**, 537 (1957).
[44] T.-P. Liu, J. Math. Anal. Appl. **53**, 78 (1976).
[45] T.-P. Liu, Mem. Am. Math. Soc. **240**, 12 (1981).
[46] T.-P. Liu and T. Ruggeri, Acta Math. Appl. Sin. **19**, 1 (2003).
[47] P. A. Thompson and Y. Kim, Phys. Fluids **26**, 3211 (1983).
[48] P. A. Thompson, H. Chaves, G. E. A. Maier, Y. Kim, and H. Speckmann, J. Fluid Mech. **185**, 385 (1987).
[49] M. S. Cramer, J. Fluid Mech. **199**, 281 (1989).
[50] A. Mentrelli and T. Ruggeri, Supplemento Rend. Circ. Mat. Palermo **II** (78), 201 (2006).
[51] A. Mentrelli, T. Ruggeri, M. Sugiyama, and N. Zhao, Wave Motion **45**, 498 (2008).
[52] L. Pareschi, G. Puppo, and G. Russo, SIAM J. Sci. Comput. (USA) **26**, 979 (2005).
[53] A. Cheng, M. L. Klein, and C. Caccamo, Phys. Rev. Lett. **71**, 1200 (1993).
[54] M. H. J. Hagen, E. J. Meijer, G. C. A. M. Mooij, D. Frenkel, and H. N. W. Lekkerkerker, Nature (London) **365**, 425 (1993).
[55] L. Mederos and G. Navascués, Phys. Rev. B **50**, 1301 (1994).
[56] Y. Zheng, N. Zhao, T. Ruggeri, M. Sugiyama, and S. Taniguchi (unpublished).